Med Biol Eng Comput
DOI 10.1007/s11517-012-1026-1

ORIGINAL ARTICLE

Evaluation of feature extraction methods for EEG-based brain–computer interfaces in terms of robustness to slight changes in electrode locations

Sun-Ae Park · Han-Jeong Hwang · Jeong-Hwan Lim · Jong-Ho Choi · Hyun-Kyo Jung · Chang-Hwan Im

Received: 13 August 2012 / Accepted: 22 December 2012

Abstract To date, most EEG-based brain–computer interface (BCI) studies have focused only on enhancing BCI performance in such areas as classification accuracy and information transfer rate. In practice, however, test–retest reliability of the developed BCI systems must also be considered for use in long-term, daily life applications. One factor that can affect the reliability of BCI systems is the slight displacement of EEG electrode locations that often occurs due to the removal and reattachment of recording electrodes. The aim of this study was to evaluate and compare various feature extraction methods for motor-imagery-based BCI in terms of robustness to slight changes in electrode locations. To this end, EEG signals were recorded from three reference electrodes (Fz, C3, and C4) and from six additional electrodes located close to the reference electrodes with a 1-cm inter-electrode distance. Eight healthy participants underwent 180 trials of left- and right-hand motor imagery tasks. The performance of four different feature extraction methods [power spectral density (PSD), phase locking value (PLV), a combination of PSD and PLV, and cross-correlation (CC)] were evaluated using five-fold cross-validation and linear discriminant analysis, in terms of robustness to electrode location changes as well as regarding absolute classification accuracy. The quantitative evaluation results demonstrated that the use of either PSD- or CC-based features led to higher classification accuracy than the use of PLV-based features, while PSD-based features showed much higher sensitivity to changes in EEG electrode location than CC- or PLV-based features. Our results suggest that CC can be used as a promising feature extraction method in motor-imagery-based BCI studies, since it provides high classification accuracy along with being little affected by slight changes in the EEG electrode locations.

Keywords Brain–computer interface (BCI) · Electroencephalography (EEG) · Electrode-location robustness (ELR), cross-correlation (CC) · Power spectral density (PSD) · Phase locking value (PLV)

1 Introduction

Brain–computer interface [BCI or brain–machine interface (BMI)] is an emerging technology that provides the disabled with a new output pathway through which they can communicate with the outside world [37]. BCI translates neural signals into specific commands for use in various daily life applications, such as wheelchair or robotic arm controllers and mental spellers [2, 8, 19, 27, 29]. Over the past few decades, BCI has been actively studied using a variety of neural signal recording modalities, such as electroencephalography (EEG) [14, 23], microelectrode arrays (MEAs) [20], electrocorticography (ECoG) [30], functional magnetic resonance imaging (fMRI) [36], and near-infrared spectroscopy (NIRS) [9]. Among these modalities, EEG-based BCI has been most widely studied due to its non-invasiveness and reasonable cost [6, 12, 18, 25, 27, 30]. Diverse types of brain electrical activities have

S.-A. Park and H.-J. Hwang are co-first authors.

S.-A. Park · J.-H. Choi · H.-K. Jung
Department of Electrical Engineering and Computer Science, Seoul National University, Seoul 133-791, Republic of Korea

H.-J. Hwang · J.-H. Lim · C.-H. Im (✉)
Department of Biomedical Engineering, Hanyang University, 222 Wangsimni-ro, Seongdong-gu, Seoul 133-791, Republic of Korea
e-mail: ich@hanyang.ac.kr

Published online: 17 January 2013

been used to materialize EEG-based BCI systems, e.g., sensorimotor rhythm [3, 7, 25], slow cortical potential [2], event-related p300 [1, 13], and steady-state visual evoked potential [21].

One of the most widely studied EEG-based BCI paradigms is the motor-imagery-based BCI. Motor imagery (MI) is defined as an imagining of kinesthetic movements, and it is well known to modulate sensorimotor rhythm around the motor cortex in the same way that actual motor execution does [31, 34]. In particular, event-related desynchronization (ERD) and event-related synchronization (ERS) of sensorimotor rhythm have been adopted as useful features for classifying different MI tasks [22, 24, 26, 27, 34]. The most commonly used feature is a time–frequency feature generally denoted as the power spectral density (PSD) feature [18]. Recently, phase locking value (PLV), a metric to measure functional connectivity between two neural signals, was introduced as a new promising feature for the MI-based BCI. A series of recent studies [5, 11] have demonstrated that PLV-based features can enhance the overall performance of MI-based BCI, especially when they are combined with conventional PSD features.

To date, most MI-based BCI studies have focused on enhancing classification accuracy and information transfer rate (ITR) [22, 24, 26, 27, 30]. Although detecting users' intentions with high classification accuracy is the primary goal, the (test–retest) reliability of the developed BCI system should also be high, so that the system can be employed in long-term, daily use applications. One important factor that can influence the reliability of a BCI system is its sensitivity to slight changes in the electrode locations, which are generally inevitable because it is difficult to attach EEG electrodes at exactly the same scalp location each time. Indeed, some previous studies have reported changes in the patterns of brain sensorimotor rhythms due to variations in the electrode locations, which can degrade BCI performance in sessions performed on different days [10, 28, 38]. However, while various feature extraction methods have been adopted to enhance the performance of MI-based BCI systems, no studies have yet investigated which feature is most robust to slight changes in electrode positions.

The goal of the present study was to discover an optimal feature extraction method that minimizes variations in classification accuracy due to slight changes in electrode positions while maintaining high classification accuracy. To this end, EEG signals were acquired from eight participants while they were performing kinesthetic motor imagery of their left and right hands. The EEG signals were acquired from three electrodes attached at Fz, C3, and C4, and from six electrodes around C3 and C4 at a 1-cm distance from C3 or C4. We evaluated four different feature extraction methods, PSD, PLV, a combination of PSD and PLV, and cross-correlation (CC), in terms of both the robustness to slight changes in electrode positions and the classification accuracy.

2 Method

2.1 Participants

Eight healthy BCI-naive volunteers (6 males and 2 females, aged 19–30 years) took part in this study. None had any history of neurological, psychiatric, or other disease that might affect the experimental results. Before the experiment, a detailed explanation of the experimental procedures was given to each participant, and all participants signed a written consent. The participants received monetary reimbursement for their participation after the experiment. The study protocol was reviewed and approved by the Institutional Review Board (IRB) of Hanyang University, Korea.

2.2 Experimental paradigm

Figure 1 shows the overall experimental procedure, which was identical to that of our previous study reported in [14]. At the beginning of each trial, a blank screen with gray (RGB: 132, 132, 132) background was presented for 3.0 s, and then a circle with a black-and-white checkerboard pattern appeared randomly on either the left or right side of the screen for the next 0.25 s to indicate which hand movement the participant was directed to imagine. Then, after a 1.0-s preparation time (blank screen), a letter X appeared at the center of the screen for 0.25 s to signal the participant to start performing the previously indicated left- or right-hand MI for the next 5.0 s. This procedure was

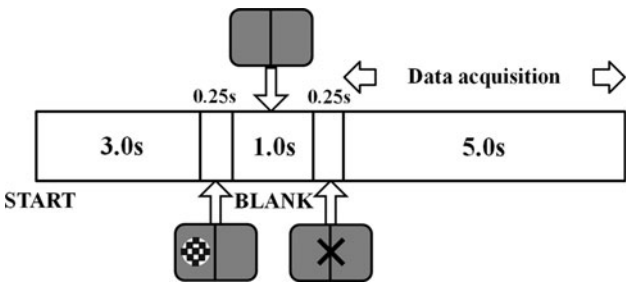

Fig. 1 The experimental paradigm used for the EEG recording. First, a blank screen was presented for 3.0 s, after which a circle with a *black*-and-*white* checkerboard pattern appeared randomly on either the *left* or *right* side of the screen for the next 0.25 s, indicating which hand movement the participant was to imagine. After a 1.0-s preparation time, the letter *X* appeared at the center of the screen for 0.25 s as a signal to start performing either *left*- or *right*-hand motor imagery. The time period used for the analyses (5.0 s) is marked on the illustration

repeated 180 times, that is, the right- and left-hand MI were each performed 90 times.

2.3 EEG data acquisition

The EEG signals were acquired at nine electrode locations using a multi-channel EEG acquisition system (WEEG-32, Laxtha Inc., Daejeon, Korea). Three electrodes were attached at Fz, C3, and C4 on the participants' scalp according to the international 10–20 system, because it has been well documented that distinct brain activities associated with MI can be obtained using these electrode sites [22, 25, 27]. To investigate variations in classification accuracy caused by slight changes in the electrode positions, six additional electrodes were attached around the C3 or C4 positions, as closely as possible (the distance between C3 or C4 and each adjacent electrode was set to 1 cm). The electrode locations used in this study are illustrated schematically in Fig. 2. The recorded EEG signals were bandpass-filtered by an anti-aliasing filter with 0.7 and 50 Hz cutoffs, and then converted into digital signals with a sampling rate of 512 Hz. The ground and reference electrodes were attached on the left and right mastoids, respectively.

2.4 EEG data analysis

As briefly mentioned in the introduction section, PSD features have been used most frequently in motor-imagery-based BCI research, and PLV features have been proposed to increase classification performance of motor-imagery-based BCI systems. Most recently, some BCI studies showed the possibility that CC-based features can be utilized as one of the useful feature types in discriminating different motor imagery tasks [32, 33]. Since the main goal of this study was to find an optimal feature type that shows stable and high classification performance regardless of slight changes in electrode positions, we used all the mentioned three feature types and thereby constructed four different kinds of feature sets, i.e., PSD, PVL, a combination of PSD and PLV, and CC.

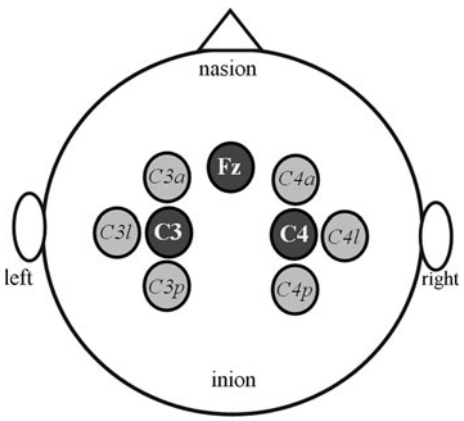

Fig. 2 EEG electrode locations used in our experiments. Locations C3, C4, and Fz were used for the training set, and six other electrodes were attached around C3 or C4 locations to acquire datasets for testing robustness to slight changes in electrode locations. The characters *a*, *l*, and *p* in the channel names represent anterior, lateral, and posterior, respectively

For the feature extraction, the 5.0-s time epoch marked in Fig. 1 was extracted for each trial. The raw EEG signals were bandpass-filtered at 8–30 Hz cutoffs, to include the mu and beta bands that are known to be closely related to MI tasks [14].

PSD features were evaluated using fast Fourier transformation (FFT) at 23 frequency bands evenly divided with frequency spans of 1 Hz [14]. The PSD features were evaluated not only for the original electrode locations (Fz, C3, and C4), but also for the six additional electrode locations (*C3a*, *C3l*, *C3p*, *C4a*, *C4l*, and *C4p*). The dimension of the constructed feature vector was 180 (90 trials for each hand's MI) by 23 (23 frequency bins) for each channel signal of each trial.

PLV features [5, 11, 17] were also extracted for all possible combinations of electrode pairs (C3-Fz, C4-Fz, C3-C4, *C3a*-Fz, *C3a*-C4, *C3l*-Fz, *C3l*-C4, *C3p*-Fz, *C3p*-C4, *C4a*-Fz, *C4a*-C3, *C4l*-Fz, *C4l*-C3, *C4p*-Fz, and *C4p*-C3). In order to quantify the degree of phase synchrony between two signals, $S_x(t)$ and $S_y(t)$, we computed the instantaneous phases $\varphi_x(t)$ and $\varphi_y(t)$ using the Hilbert transform. The Hilbert transform of $S(t)$ is defined as

$$\tilde{S}(t) = \frac{1}{\pi} P.V. \int_{-\infty}^{\infty} \frac{S(\tau)}{t-\tau} d\tau \tag{1}$$

where, $\tilde{S}(t)$ is the Hilbert transform of the time series $S(t)$, and $P.V.$ denotes the Cauchy principal value. The instantaneous phase $\varphi(t)$ can then be estimated as

$$\varphi(t) = \arctan \frac{\tilde{S}(t)}{S(t)} \tag{2}$$

The PLV was evaluated using the following definition:

$$PLV = \left| \left\langle e^{j\Delta\varphi(t)} \right\rangle \right| \tag{3}$$

where, $\Delta\varphi(t) = \varphi_x(t) - \varphi_y(t)$, and $|\langle\cdot\rangle|$ is the averaging operator. When estimating PLV features, we used the identical frequency band and time window used for extracting the PSD features. To construct the feature set consisting of both PSD and PLV features, we simply combined the extracted PLV features with the PSD features.

To extract the CC features, Fz was selected as the reference channel because the EEG signals recorded at Fz are less affected by the left- and right-hand MI than those

recorded at C3 and C4. In order to extract the CC features associated with the left-hand MI task, EEG signals recorded at C3 and C4 were cross-correlated with the reference EEG signal at Fz, resulting in two CC sequences for C3 and C4 (see Fig. 4 depicting some examples of the CC sequences). Six statistical features (mean, standard deviation, skewness, kurtosis, and maximum and minimum values) were then extracted from each CC sequence to characterize the distribution of CC sequences as well as to reduce the dimensions of the feature vector [32, 33]. The same procedure was repeated for each trial of right-hand MI. For more detailed description of the process, please refer to the previous literatures [32, 33].

The best feature subsets for each feature vector were selected using a sequential feature selection (SFS) algorithm [15], with the number of selected features limited to 10 to avoid over-fitting of the training data. As some BCI studies reported that a linear discriminant analysis (LDA) algorithm showed high and stable classification performance as compared to other classification methods used in motor-imagery-based BCI research [4, 35], we used the LDA algorithm in this study. A five-fold cross-validation method was used to avoid biases in estimating classification accuracy. For each of the five cross-validation processes, we used training data (4/5 of all trials) obtained from one dataset (Fz, C3, C4), and we used test data (remaining 1/5 trials) from seven different test datasets (Fz, C3, C4), (Fz, *C3a*, C4), (Fz, *C3l*, C4), (Fz, *C3p*, C4), (Fz, C3, *C4a*), (Fz, C3, *C4l*), and (Fz, C3, *C4p*), to investigate variations in classification accuracy related to changes in the electrode locations.

2.5 An index to quantify robustness to electrode location changes: ELR

To quantify variations in classification accuracy due to slight changes in the electrode locations, we introduced a new index, the electrode location robustness (ELR) metric. The ELR was defined as

$$\begin{aligned} &\mathrm{ELR} = \frac{1}{6}\sum_{(i,j)} |CA_{\mathrm{Fz,C3,C4}} - CA_{\mathrm{Fz},i,j}|, \\ &(i,j) = (C3a,\mathrm{C4}),(C3l,\mathrm{C4}),(C3p,\mathrm{C4}),(\mathrm{C3},C4a), \\ &(\mathrm{C3},C4l),\ \text{and}\ (\mathrm{C3},C4p), \end{aligned} \tag{4}$$

where $CA_{\mathrm{Fz},i,j}$ represents the classification accuracy estimated from five-fold cross-validation when EEG signals recorded from three electrodes, Fz, *i*, and *j*, are used for the test dataset. For example, in Table 1, the ELR value can be simply evaluated by averaging absolute differences between first row (Fz, C3, C4) and each of the other six rows. An ELR value of zero would indicate that classification accuracy is not at all affected by changes in the electrode locations, while a high ELR value would indicate that slight changes in the electrode locations strongly influence classification accuracy. Therefore, the ELR can directly quantify variations of classification accuracy caused by slight changes in the electrode locations.

3 Results

Table 1 shows the average classification accuracy evaluated for four different feature extraction methods. The classification accuracies for PSD feature sets were relatively higher than those for PLV feature sets, in all electrode combinations. Meanwhile, simultaneous use of both PSD and PLV features led to higher classification accuracies than with PSD alone. These results are in line with previous MI-based BCI studies [5, 11], in which the performances of PSD, PLV, and PSD + PLV features were compared in terms of classification accuracy. Results also show that the classification accuracy using CC features was higher than with any of the other three methods, regardless

Table 1 Classification accuracy averaged over all participants

Electrode combination of test dataset	Average classification accuracy (%) (standard deviation)			
	PSD	PLV	PSD + PLV	CC
Fz, C3, C4	82.70 (7.66)	67.36 (12.60)	83.49 (7.11)	89.20 (6.24)
Fz, C3, C4a	83.33 (6.08)	67.51 (11.84)	85.62 (5.05)	86.77 (10.76)
Fz, C3, C4l	82.98 (5.28)	68.68 (12.08)	85.76 (5.20)	87.84 (8.73)
Fz, C3, C4p	81.94 (6.09)	67.84 (11.08)	84.93 (4.31)	88.54 (8.23)
Fz, C3a, C4	79.30 (5.28)	66.73 (10.46)	80.69 (6.66)	89.00 (5.87)
Fz, C3l, C4	75.76 (6.87)	68.05 (13.20)	79.23 (9.44)	87.99 (6.98)
Fz, C3p, C4	76.52 (6.10)	67.29 (11.36)	78.75 (9.58)	87.47 (5.48)

For each five-fold cross validation, a training dataset (4/5 of all trials) was obtained from the (Fz, C3, C4) combination, and seven different test datasets (remaining 1/5 trials) obtained from (Fz, C3, C4), (Fz, *C3a*, C4), (Fz, *C3l*, C4), (Fz, *C3p*, C4), (Fz, C3, *C4a*), (Fz, C3, *C4l*), and (Fz, C3, *C4p*) were tested

of the electrode locations, which is also consistent with results reported previously [32, 33].

Table 2 summarizes the ELR values of all participants. It can be observed from the table that CC and PLV features are relatively less affected by slight changes in the electrode locations than the other two features. Statistical testing (RM-ANOVA) results also confirmed significant difference between PSD-based features and CC/PLV-based features [RM-ANOVA: $F(3, 21) = 4.63$, $p = 0.0123$; post hoc analysis (paired t test): PSD = PSD + PLV > PLV = CC, corrected $p < 0.01$]. To confirm these results more intuitively, the classification accuracy and ELR values of each participant are illustrated in Fig. 3. The figure clearly shows that the CC features outperform the other three kinds of features in terms of classification accuracy. CC features show similar ELR distributions to PLV features, but CC features show much better classification performance than PLV features.

Table 2 Electrode location robustness (ELR) metric of all participants

Electrode location robustness (ELR) metric				
Subject no.	Feature extraction methods			
	PSD	PLV	PSD + PLV	CC
S1	2.685	2.126	5.00	2.13
S2	5.65	2.85	6.66	2.15
S3	8.98	2.86	6.94	1.47
S4	15.92	2.87	2.22	3.5
S5	2.963	1.76	2.68	2.68
S6	6.11	4.075	2.68	4.1
S7	4.258	1.39	3.88	3.37
S8	6.018	2.4	6.35	3.17
Average	6.57 (4.277)	2.54 (0.827)	4.55 (1.944)	2.82 (0.870)

Lower ELR values indicate that the classification accuracy is less affected by slight changes in the electrode locations

Figure 4 shows examples of cross-correlation sequences of two participants (subjects 4 and 5) evaluated between four electrodes (C3, C3a, C3l, and C3p) and a reference electrode (Fz). The cross-correlation sequences for the left- and right-hand MI showed very clear differences in shape, leading to high accuracy in classifying the two different MI tasks. It can also be clearly observed from the figures that the overall shapes of the cross-correlation sequences are not changed much by the slight changes in the electrode locations, which ultimately led to small ELR values in our results.

Figure 5 shows examples of PSD results of two participants (subjects 4 and 5) evaluated at four electrodes (C4, *C4a*, *C4l*, and *C4p*). The PSD values for the left- and right-hand MI showed clear differences around the mu rhythm (8–12 Hz), as has been frequently reported in the literature [22, 24, 26, 27, 30]. In contrast to the CC plots in Fig. 4, however, the PSD values within the mu frequency band significantly varied with changes in the electrode locations, leading to the high ELR values in our analysis results.

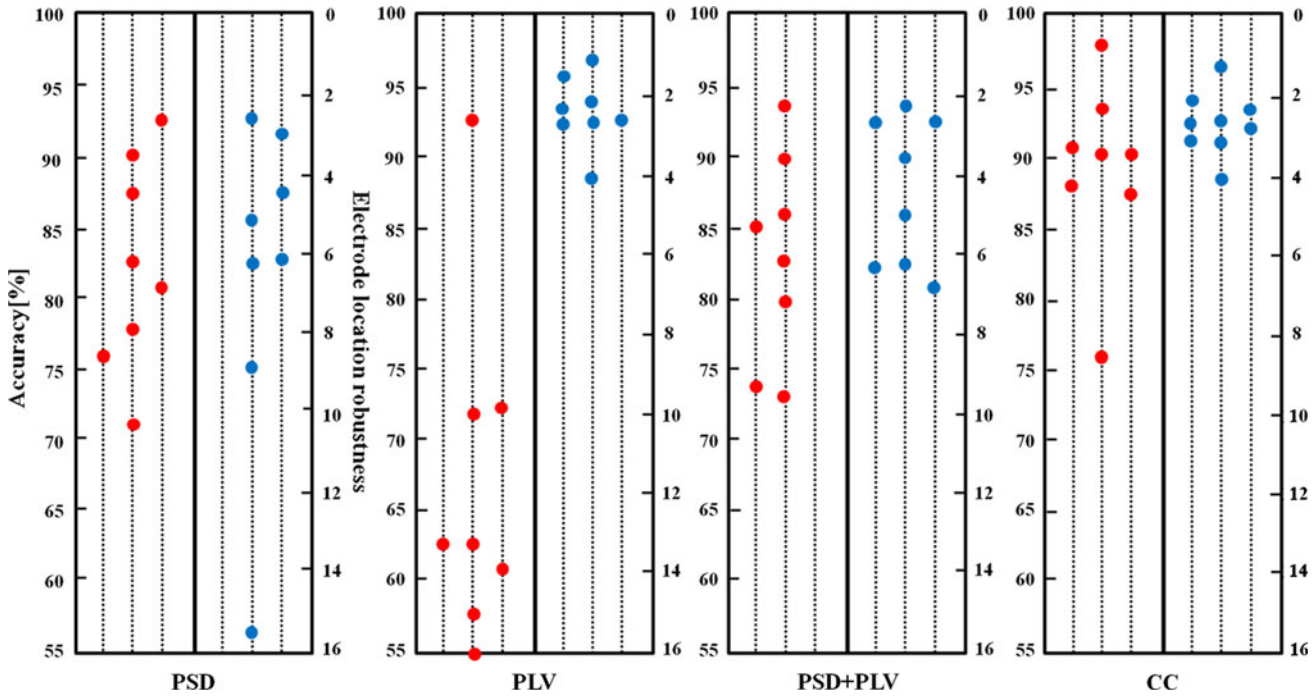

Fig. 3 Classification accuracy (*left* part of each plot) and ELR (*right* part of each plot) distributions of all participants

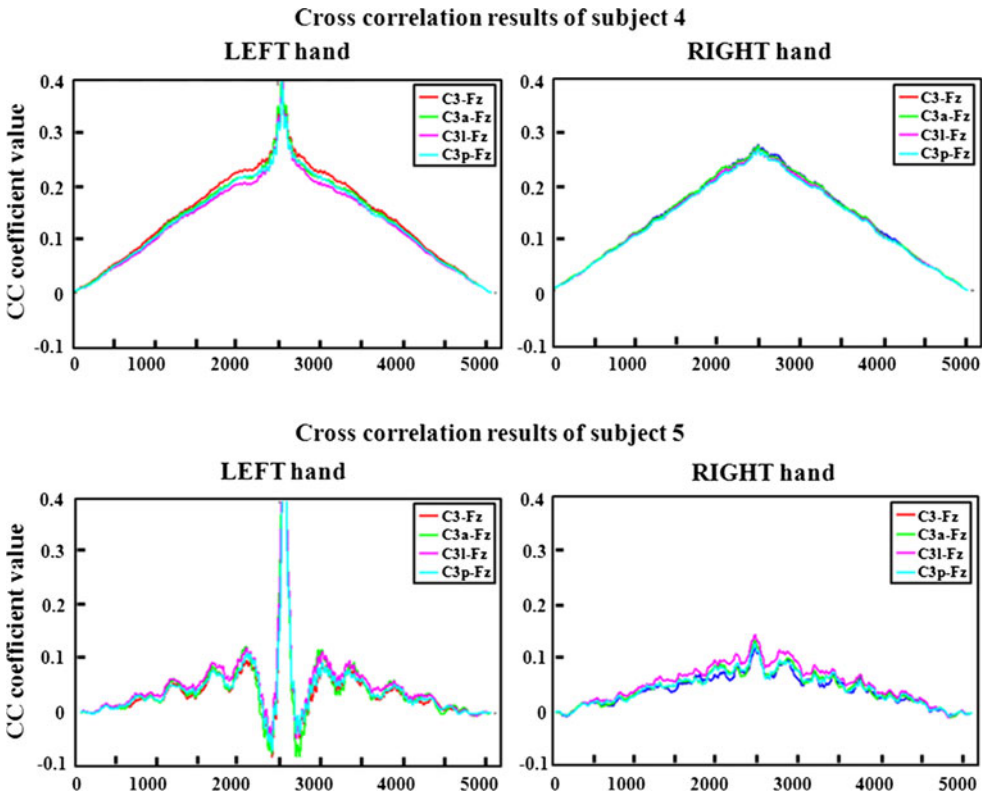

Fig. 4 Examples of cross-correlation sequences for two participants (subjects 4 and 5) evaluated between four electrodes (C3, *C3a*, *C3l*, and *C3p*) and a reference electrode (Fz). "*LEFT hand*" and "*RIGHT hand*" indicate left- and right-hand motor imagery, respectively

Figure 6 depicts examples of PLV results of two participants (subject 4 and 5) estimated between four electrodes (C4, C*4a*, C*4l*, and C*4p*) and a reference electrode (Fz). The distributions of the PLV values for the left- and right-hand MI were very similar in all frequencies (8–30 Hz), thereby leading to relatively low classification performance as compared to the other three feature sets. However, as similar to the CC plots in Fig. 4, the PLV values were less affected by slight changes in electrode positions, which resulted in small ELR values as presented in Table 2.

4 Discussion

Since it is difficult in practice to permanently affix EEG electrodes on an individual's scalp, there are inevitably subtle changes in the electrode locations after removing and reattaching them. In the current study, various feature extraction methods were evaluated in terms of robustness to electrode location changes. To our knowledge, no previous study has attempted to quantitatively evaluate the variations in classification accuracy caused by slight changes in the electrode locations. To date, the vast majority of MI-based BCI systems have relied on features derived from band PSD evaluation. Recently, features derived from PLV calculations have shown improved classification accuracy when combined with those extracted from PSD evaluation. Our analyses of EEG datasets acquired from eight participants demonstrated that CC features provided better BCI performances in terms of both electrode location robustness and classification accuracy than the other feature extraction methods: PSD, PLV, and their combination. According to a previous study [32, 33], techniques using CC features can diminish noises effectively thanks to the characteristics of signal periodicity, and they are also free from loss of information resulting from frequency domain transformation. Our results further suggest that CC should be considered as a new promising feature in future MI-based BCI studies.

One of the main findings in our study was the confirmation that PLV and CC features were less affected by slight changes in the electrode locations than were PSD features, as expected. When an electrode location is moved in a certain direction, the magnitude of the spectral power changes accordingly, leading to changes in classification accuracy when using PSD-based features. Indeed, PSD values around the mu band (8–12 Hz) fluctuated significantly according to changes in electrode locations, as shown in Fig. 5. In contrast, CC features are not affected by simple scaling of signal amplitude as shown in Fig. 4. According to Lachaux et al.'s study [17], PLV features can be influenced by changes in electrode locations, but the absolute PLV values are linearly changed with respect to the distance between two electrodes. In our study, we could also observe this characteristic from Fig. 6, in which PLV

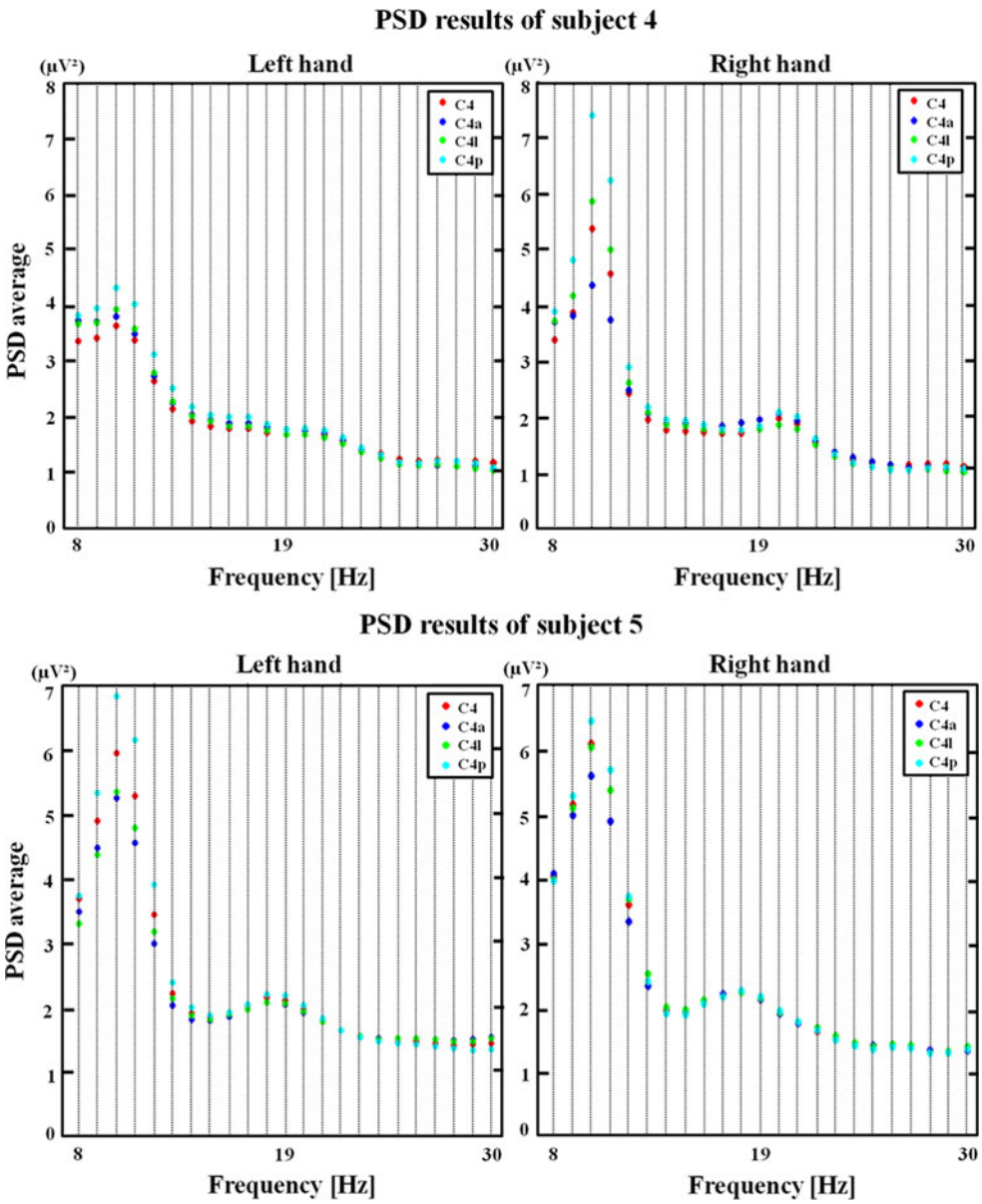

Fig. 5 Examples of power spectral density (PSD) results for two participants (subjects 4 and 5) evaluated at four electrodes (C4, *C4a*, *C4l*, and *C4p*). "*LEFT hand*" and "*RIGHT hand*" indicate left- and right-hand motor imagery, respectively

values were almost linearly changed when electrode positions were moved from an original position (C4). Since the neural electrical source of MI is generally restricted to the sensorimotor cortex, slight displacement of an electrode rarely affects the characteristics of phase information and signal waveform of a signal, thereby resulting in relatively little degradation of classification accuracy when using PLV and CC features. Although 1 cm displacement of electrode locations is thought to be sufficiently large in practical cases, investigations on the changes in three feature sets due to the electrode location shifts larger than 1 cm would be an interesting future research topic.

Our experiments have a few limitations. In our study, certain EEG electrodes were attached at scalp locations 1 cm away from C3 or C4 locations. We chose 1 cm as the inter-electrode distance because the disk-type electrodes used in our study had radii of 0.3 cm, and a sufficient distance between two adjacent electrodes was needed to prevent them from being electrically connected. In addition, we assumed the Fz electrode was not displaced, because the Fz location can be relatively accurately determined since it is on the midline. Our experiments were restricted to only motor imagery tasks, and our investigation needs to be extended to other types of mental imagery tasks used for implementing BCI systems, such as mental arithmetic, internal singing, mental word composition, and so on. In the present study, we only evaluated the effect of EEG electrodes displacement on classification accuracy, but we did not address test–retest reliability of the BCI approach, which is an interesting topic for future

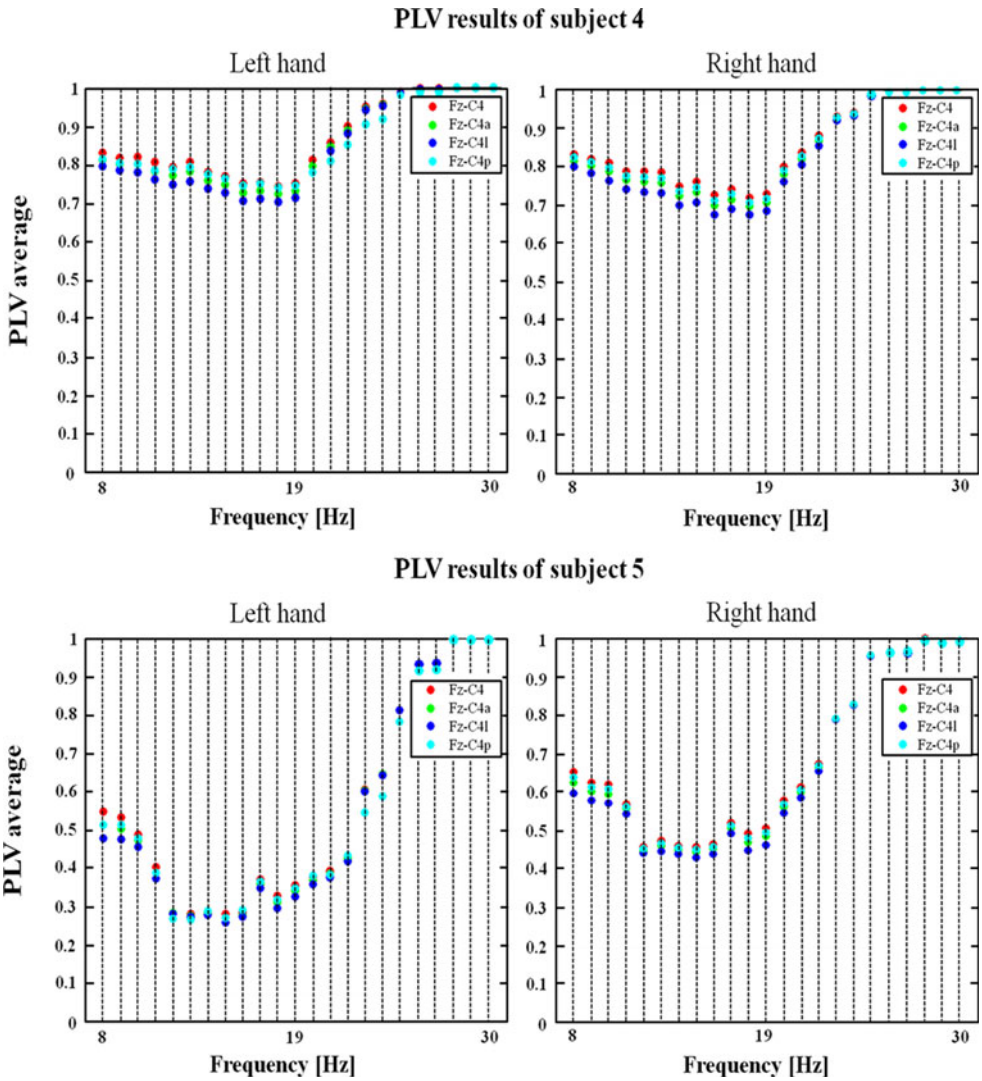

Fig. 6 Examples of phase locking value (PLV) results for two participants (subject 4 and 5) evaluated between four electrodes (C4, C4*a*, C4*l*, and C4*p*) and a reference electrode (Fz). "*LEFT hand*" and "*RIGHT hand*" indicate left- and right-hand motor imagery, respectively

explorations. In future studies, we will continue evaluating various feature extraction methods by performing longitudinal experimental studies focused on test–retest reliability.

In cases when a relatively larger number of electrodes are used for a BCI system, feature vectors extracted from source space [16] are less likely to be affected by the slight changes in electrode locations, compared to those extracted from sensor space. Therefore, investigating the robustness to electrode position shift of methods that do not work on sensor space features would be an interesting topic of future research.

5 Conclusion

In this study, we investigated four different kinds of features to find the best feature type showing consistent and high classification accuracy regardless of slight changes in electrode positions. The use of PSD-based features resulted in high classification accuracy, but showed high sensitivity to changes in the electrode locations. The use of PLV-based features showed almost opposite results to those attained using the PSD-based features. On the other hand, CC-based features provided high classification accuracy comparable to PSD features with being least affected by slight changes in the electrode locations. Our results suggest that CC can be used as a promising feature extraction method in motor-imagery-based BCI studies.

Acknowledgments This work was supported in part by the Public Welfare and Safety Research Program through the National Research Foundation of Korea (NRF) funded by the Ministry of Education, Science, and Technology (No. 2011-0027859) and in part by the Original Technology Research Program for Brain Science through a National Research Foundation of Korea (NRF) Grant funded by the Ministry of Education, Science, and Technology (No. 2012-0006331).

References

1. Bayliss JD (2003) Use of the evoked potential P3 component for control in a virtual apartment. IEEE Trans Neural Syst Rehabil Eng 11:113–116
2. Birbaumer N, Ghanayim N, Hinterberger T, Iversen I, Kotchoubey B, Kubler A, Perelmouter J, Taub E, Flor H (1999) A spelling device for the paralysed. Nature 398:297–298
3. Blankertz B, Dornhege G, Krauledat M, Muller KR, Curio G (2007) The non-invasive Berlin brain–computer interface: fast acquisition of effective performance in untrained subjects. Neuroimage 37:539–550
4. Boostani R, Graimann B, Moradi MH, Pfurtscheller G (2007) A comparison approach toward finding the best feature and classifier in cue-based BCI. Med Biol Eng Comput 45:403–412
5. Brunner C, Scherer R, Graimann B, Supp G, Pfurtscheller G (2006) Online control of a brain–computer interface using phase synchronization. IEEE Trans Biomed Eng 53:2501–2506
6. Cecotti H (2011) Spelling with non-invasive brain–computer interfaces—current and future trends. J Physiol-Paris 105:106–114
7. Chatterjee A, Aggarwal V, Ramos A, Acharya S, Thakor NV (2007) A brain–computer interface with vibrotactile biofeedback for haptic information. J NeuroEng Rehabil 4:40
8. Cong W, Bin X, Jie L, Wenlu Y, Dianyun X, Velez AC, Hong Y (2011) Motor imagery BCI-based robot arm system. In: Proceedings of the Seventh International Conference on Natural Computation (ICNC), Shanghai, China, pp 181–184
9. Coyle S, Ward T, Markham C, McDarby G (2004) On the suitability of near-infrared (NIR) systems for next-generation brain–computer interfaces. Physiol Meas 25:815–822
10. Guger C, Ramoser H, Pfurtscheller G (2000) Real-time EEG analysis with subject-specific spatial patterns for a brain–computer interface (BCI). IEEE Trans Rehabil Eng 8:447–456
11. Gysels E, Celka P (2004) Phase synchronization for the recognition of mental tasks in a brain–computer interface. IEEE Trans Neural Syst Rehabil Eng 12:406–415
12. Gysels E, Renevey P, Celka P (2005) SVM-based recursive feature elimination to compare phase synchronization computed from broadband and narrowband EEG signals in brain–computer interfaces. Signal Process 85:2178–2189
13. Hoffmann U, Vesin JM, Ebrahimi T, Diserens K (2008) An efficient P300-based brain–computer interface for disabled subjects. J Neurosci Methods 167:115–125
14. Hwang HJ, Kwon K, Im CH (2009) Neurofeedback-based motor imagery training for brain–computer interface (BCI). J Neurosci Methods 179:150–156
15. Jain A, Zongker D (1997) Feature selection: evaluation, application, and small sample performance. IEEE Trans Pattern Anal Mach Intell 19:153–158
16. Kamousi B, Liu Z, He B (2005) Classification of motor imagery tasks for brain–computer interface applications by means of two equivalent dipoles analysis. IEEE Trans Neural Syst Rehab Eng 13:166–171
17. Lachaux JP, Rodriguez E, Martinerie J, Varela FJ (1999) Measuring phase synchrony in brain signals. Hum Brain Mapp 8:194–208
18. Lotte F, Congedo M, Lecuyer A, Lamarche F, Arnaldi B (2007) A review of classification algorithms for EEG-based brain–computer interfaces. J Neural Eng 4:R1–R13
19. McFarland DJ, Wolpaw JR (2008) Brain–computer interface operation of robotic and prosthetic devices. Computer 41:52–56
20. Mellinger J, Schalk G, Braun C, Preissl H, Rosenstiel W, Birbaumer N, Kubler A (2007) An MEG-based brain–computer interface (BCI). Neuroimage 36:581–593
21. Middendorf M, McMillan G, Calhoun G, Jones KS (2000) Brain–computer interfaces based on the steady-state visual-evoked response. IEEE Trans Rehabil Eng 8:211–214
22. Neuper C, Scherer R, Reiner M, Pfurtscheller G (2005) Imagery of motor actions: differential effects of kinesthetic and visual-motor mode of imagery in single-trial EEG. Cogn Brain Res 25:668–677
23. Neuper C, Scherer R, Wriessnegger S, Pfurtscheller G (2009) Motor imagery and action observation: modulation of sensorimotor brain rhythms during mental control of a brain–computer interface. Clin Neurophysiol 120:239–247
24. Neuper C, Schlogl A, Pfurtscheller G (1999) Enhancement of left-right sensorimotor EEG differences during feedback-regulated motor imagery. J Clin Neurophysiol 16:373–382
25. Pfurtscheller G, Brunner C, Schlogl A, da Silva FHL (2006) Mu rhythm (de)synchronization and EEG single-trial classification of different motor imagery tasks. Neuroimage 31:153–159
26. Pfurtscheller G, Neuper C (2001) Motor imagery and direct brain–computer communication. Proc IEEE 89:1123–1134
27. Pfurtscheller G, Neuper C, Flotzinger D, Pregenzer M (1997) EEG-based discrimination between imagination of right and left hand movement. Electroencephalogr Clin Neurophysiol 103:642–651
28. Pfurtscheller G, Stancak A, Edlinger G (1997) On the existence of different types of central beta rhythms below 30 Hz. Electroencephalogr Clin Neurophysiol 102:316–325
29. Rebsamen B, Guan CT, Zhang HH, Wang CC, Teo C, Ang MH, Burdet E (2010) A brain controlled wheelchair to navigate in familiar environments. IEEE Trans Neural Syst Rehabil 18:590–598
30. Schalk G, Leuthardt EC (2011) Brain–computer interfaces using electrocorticographic signals. IEEE Rev Biomed Eng 4:140–154
31. Sharma N, Pomeroy VM, Baron JC (2006) Motor imagery: a backdoor to the motor system after stroke? Stroke 37:1941–1952
32. Siuly, Yan L, Jinglong W, Jingjing Y (2011) Developing a logistic regression model with cross-correlation for motor imagery signal recognition. In: Proceedings of the 2011 IEEE/ICME International Conference on Complex Medical Engineering (CME), Harbin, China, pp 502–507
33. Siuly S, Li Y (2012) Improving the separability of motor imagery EEG signals using a cross correlation-based least square support vector machine for brain–computer interface. IEEE Trans Neural Syst Rehabil 20:526–538
34. Thomas KP, Guan CT, Lau CT, Vinod AP, Ang KK (2009) A new discriminative common spatial pattern method for motor imagery brain–computer interfaces. IEEE Trans Biomed Eng 56:2730–2733
35. Vidaurre C, Scherer R, Cabeza R, Schlogl A, Pfurtscheller G (2007) Study of discriminant analysis applied to motor imagery bipolar data. Med Biol Eng Comput 45:61–68
36. Weiskopf N, Veit R, Erb M, Mathiak K, Grodd W, Goebel R, Birbaumer N (2003) Physiological self-regulation of regional brain activity using real-time functional magnetic resonance imaging (fMRI): methodology and exemplary data. Neuroimage 19:577–586
37. Wolpaw JR, Birbaumer N, Heetderks WJ, McFarland DJ, Peckham PH, Schalk G, Donchin E, Quatrano LA, Robinson CJ, Vaughan TM (2000) Brain–computer interface technology: a review of the first international meeting. IEEE Trans Rehabil Eng 8:164–173
38. Wolpaw JR, McFarland DJ, Vaughan TM (2000) Brain–computer interface research at the Wadsworth Center. IEEE Trans Rehabil Eng 8:222–226